



University of Warwick institutional repository: <http://go.warwick.ac.uk/wrap>

This paper is made available online in accordance with publisher policies. Please scroll down to view the document itself. Please refer to the repository record for this item and our policy information available from the repository home page for further information.

To see the final version of this paper please visit the publisher's website. Access to the published version may require a subscription.

Author(s): O. A. Mironov, M. Goiran, J. Galibert, D. V. Kozlov, A. V. Ikonnikov, K. E. Spirin, V. I. Gavrilenko, G. Isella, M. Kummer, H. von Känel, O. Drachenko, M. Helm, J. Wosnitza, R. J. H. Morris and D. R. Leadley

Article Title: Cyclotron Resonance of Extremely Conductive 2D Holes in High Ge Content Strained Heterostructures

Year of publication: 2010

Link to published version:

<http://dx.doi.org/10.1007/s10909-009-0147-x>

Publisher statement: The original publication is available at www.springerlink.com

O.A. Mironov¹, M. Goiran², J. Galibert²,
D.V. Kozlov³, A.V. Ikonnikov³, K.E. Spirin³,
V.I. Gavrilenko³, G. Isella⁴, M. Kummer⁴,
H. von Känel⁴, O. Drachenko⁵, M. Helm⁵,
J. Wosnitza⁵, R.J.H. Morris⁶ and D.R. Leadley⁶

Cyclotron resonance of extremely conductive 2D holes in high Ge content strained heterostructures

1.06.2009

Abstract Cyclotron resonance has been observed in steady and pulsed magnetic fields from high conductivity holes in Ge quantum wells. The resonance positions, splittings and linewidths are compared to calculations of the hole Landau levels.

Keywords cyclotron resonance, quantum well, effective mass, Landau level

PACS 72.20.Ht, 72.20.My, 73.23.-b

The mobility of a two-dimensional hole gas (2DHG) in strained germanium can be much higher than in silicon and extremely conductive layers can be formed where there is also a high hole density p_s . Here we have investigated highly conductive “pure Ge” strained channels in quantum wells (QW) by a combination of cyclotron resonance (CR) and magneto-transport (MT) in quasi-static and pulsed magnetic fields B and compared the results with calculations of the energy levels. Two epitaxial techniques were used to grow the layers, with carriers introduced by modulation doping from one side. Sample 68072 was produced by a *hybrid-epitaxy*¹ that combines UHV-CVD for the $\text{Si}_{0.4}\text{Ge}_{0.6}$ strain-tuning buffer and low temperature SS-MBE for the 20 nm thick “Ge” channel. Low field Hall measurements showed a hole mobility of 27,000 cm^2/Vs at a sheet density $p_s = 2 \times 10^{12} \text{cm}^{-2}$, which represents a higher conductance than other “high-Ge”

1: Warwick SEMINANO R&D Centre, University of Warwick Science Park, The Venture Centre, Coventry CV4 7EZ, UK; International Laboratory of High Magnetic Fields and Low Temperatures, P.O. Box 4714, 50-985 Wrocław 47, Poland

2: Laboratoire Nationale des Champs Magnetiques Pulses, Universite de Toulouse, 143 av. de Rangueil, 31432, Toulouse, France

3: Institute for Physics of Microstructures, RAS, Nizhny Novgorod 603950, Russia

4: Laboratorium für Festkörperphysik, ETH Zürich, CH-8093 Zürich; EpiSpeed AG, Technoparkstrasse 1, CH-8005 Zurich, Switzerland; L-NESS and Dipartimento di Fisica del Politecnico di Milano, I-22100 Como, Italy.

5: Dresden High Magnetic Field Laboratory and Institute of Ion-Beam Physics and Materials Research, Forschungszentrum Dresden-Rossendorf, P.O. Box 510119, 01314 Dresden, Germany

6: Department of Physics, University of Warwick, Coventry CV4 7AL, UK

E-mail: d.r.leadley@warwick.ac.uk

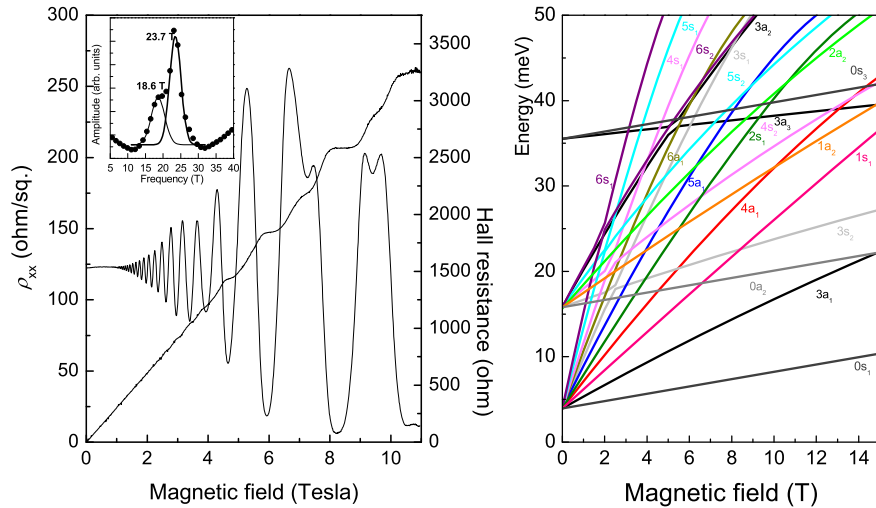


Fig. 1 (Left) MR measurements for sample 68072 at $T = 1$ K. Inset: FFT of SdHOs showing two subband occupation.

Fig. 2 (Right) Calculated LLs in sample 68072 for the three lowest electric subbands.

heterostructures. MT measurements at $T = 0.9$ K are presented in Fig.1 and clearly show Shubnikov-de Haas oscillations (SdHO) and quantum Hall plateaux. One can also see the effect of SdHO “beating” that indicates holes are occupying the second electric subband. Fast Fourier Transform analysis of the magnetoresistance data in inverse magnetic field (Fig.1 inset) gives a sheet density of $1.1 \times 10^{12} \text{cm}^{-2}$ and $8.9 \times 10^{11} \text{cm}^{-2}$ in the 1st and 2nd subbands, respectively. Sample K6043 was grown by LEPE-CVD² with a 25 nm thick “Ge” QW on a $\text{Si}_{0.3}\text{Ge}_{0.7}$ buffer and had a DC Van der Pauw mobility of $68,000 \text{cm}^2/\text{Vs}$ at $p_s = 4.4 \times 10^{11} \text{cm}^{-2}$. The lower Si content in the buffer means that this sample has less strain in the channel. We should point out that in each case the “Ge” quantum wells in fact contained a small amount (2-5%) of Si.

CR measurements in quasi-static magnetic fields used a Bruker 113V FT spectrometer at Grenoble HMFL. The radiation transmitted through the sample was detected with a Si composite bolometer and signals obtained in magnetic fields were normalized to the zero field values. CR measurements were also made in pulsed magnetic fields at LNCMP/Toulouse with a CO_2 -pumped FIR gas laser source. The pulse energy of 1.2 MJ produced a peak field of 40 T, with a duration of 800 ms. A light pipe guided the radiation into a liquid helium cryostat inserted in the bore of the pulsed solenoid, with the transmitted radiation being detected by either an n-InSb or Ge photodetector. Very good CR lines were obtained for all the samples tested across the wavelength range $70 \mu\text{m} < \lambda < 871 \mu\text{m}$ and for temperatures 1.8 – 200 K, although we only refer to the lowest temperatures here. By using 40 T pulsed fields we could ensure the absence of CR transitions at higher fields that could result from transitions between higher LLs. Although we only report on transitions up to 15 T here, this work establishes the methodology that we have subsequently applied to other samples using higher laser frequencies.

To interpret the measured CR spectra, we have developed a model based on a 4×4 Luttinger Hamiltonian that includes the deformation potential and the rectangular QW energy profile. For these Ge quantum wells the spin orbit splitting of 280 meV far exceeds the hole Fermi energy (25-40 meV) so we do not need a more

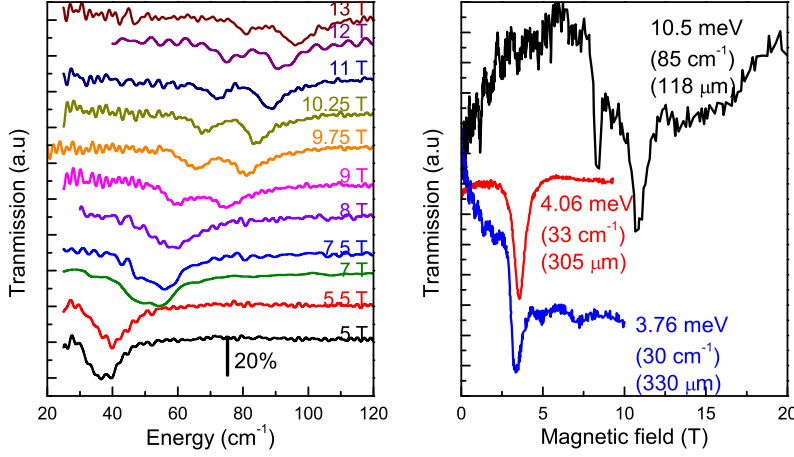


Fig. 3 (Left) CR spectra for sample 68072 at $T = 1.8$ K in static magnetic fields.

Fig. 4 (Right) CR spectra for sample K6043 at $T = 4.2$ K in pulsed magnetic fields.

complex 6×6 Hamiltonian.³ The eigenfunctions of the Hamiltonian were calculated in a vector-potential gauge given by $\mathbf{A} = \frac{1}{2}[\mathbf{H} \times \mathbf{r}]$. The Luttinger parameters for the SiGe alloy were interpolated linearly between the Ge and Si values. We also neglected the off-diagonal terms in the Hamiltonian, proportional to $(\gamma_2 - \gamma_3)$, *i.e.* anisotropy in the QW plane was not taken into account (the axial approximation). Additionally, low field effective cyclotron masses were determined as a function of 2DHG concentration, to be compared with the MT mass values.

The Landau levels (LLs) calculated for sample 68072 are presented in Fig.2 and are characterized by a quantum number n (a kind of LL index), a wave function parity: a -antisymmetric, s - symmetric, and the index i which labels the electric subband.⁴ The selection rules allow CR transitions for $\Delta n = 1$ between LLs of the same parity and belonging to the same electric subband. For example, at $B = 11$ T eight LLs are occupied in sample 68072 (see the prominent quantum Hall plateau between 10.5 and 11 T in Fig.1). The last filled LL at 11 T is labelled $4s_2$ in Fig.2, therefore the allowed CR transitions (between filled and empty LLs) are $4s_2 \rightarrow 5s_2$ (10.2 meV) and $1a_2 \rightarrow 2a_2$ (9.3 meV) within the 2nd subband, and $4a_1 \rightarrow 5a_1$ (13.3 meV) and $1s_1 \rightarrow 2s_1$ (15 meV) within the 1st subband.

Typical CR spectra from sample 68072 are shown in Fig.3. For low magnetic fields the observed CR line position corresponds to an effective cyclotron mass $m_c^* = 0.12m_0$, which coincides with the calculated CR effective mass in the 1st electric subband (at $p_{s1} = 1.1 \times 10^{12} \text{ cm}^{-2}$). However, the calculated effective mass in the 2nd electric subband (at $p_{s2} = 0.89 \times 10^{11} \text{ cm}^{-2}$) is much higher at $0.147m_0$, which means CR transitions from these two subbands will occur at different fields leading to significant CR line broadening.

In high magnetic fields, over 8 T, a prominent CR line splitting was observed due to the different LL spacing in the two electric subbands. This contrasts with Ref. 5 where CR line splitting was observed in a similar SiGe/Ge heterostructure, with a lower 2DHG concentration, due only to differences in the 1st subband. The observed positions of the lower frequency CR absorption line correspond fairly well to the calculated energies of the allowed CR transitions within the 2nd subband, mentioned above; however, the photon energies corresponding to the higher frequency peak are 20 to 25% less than the calculated transition energies

in the first electric subband. A possible reason for this disagreement is that band bending due to the single side modulation doping has not been taken into account in the model. This will make the well more asymmetric, raising the 1st subband significantly, but with correspondingly less effect on higher subbands. In each case only one broad feature is observed per subband, rather than resolving the two different calculated energies.

Fig.4 shows CR spectra measured in pulsed magnetic fields at 3 different FIR wavelengths for sample K6043. At long wavelengths the resonant magnetic fields correspond to a low CR effective mass of $m_c^* = 0.10m_0$ that obviously results from the low 2DHG concentration of $4.4 \times 10^{11} \text{cm}^{-2}$. This is in good agreement with $m^* = (0.820.07)m_0$ measured from SdHO.⁷ By contrast, at the shorter wavelength of $\lambda = 118 \mu\text{m}$ two CR lines are clearly observed. These have a quite different origin from the splitting observed for sample 68072 in Fig.3, since only the two lowest hole LLs, $0s_1$ and $3a_1$ in the lowest electric subband, are occupied between 8.5 and 10.8 T in K6043. According to the selection rules, the transition at $B = 8.5$ T must be the $0s_1 \rightarrow 1s_1$ transition while that $B = 10.8$ T corresponds to $3a_1 \rightarrow 4a_1$; however, the FIR photon energy is much less (by 50%) than the calculated separation of the corresponding LLs. This large discrepancy shows that the evolution of LLs in magnetic field for the two samples are significantly different and could result from the different amounts of strain and Si segregation in the QW.

Mobility values were also obtained from the CR linewidth measured in pulsed fields for both samples. For sample 68072, the FWHM at $\lambda = 305 \mu\text{m}$ corresponds to a mobility of $1.5 \times 10^4 \text{cm}^2/\text{Vs}$ that is only half the measured DC mobility of $2.7 \times 10^4 \text{cm}^2/\text{Vs}$, because of CR line broadening due to the different effective masses in each subband. Since the line widths in pulsed and quasistatic fields (from Fig.3) agree, RC time constants in the transient recording are not the source of additional broadening. For sample K6043 with only the 1st subband occupied, the CR FWHM at $\lambda = 305 \mu\text{m}$ corresponds to a mobility of $2.9 \times 10^4 \text{cm}^2/\text{Vs}$ that again is only half the DC mobility value. The origin of the discrepancy in this case seems to be quite different; at the resonant magnetic field of 3.6 T several hole LLs are occupied and the CR linewidth is governed by a non-equidistant LL spacing as well as individual LL widths, which are determined by the single particle quantum lifetime rather than the transport (momentum relaxation) time that can be 5 – 8 times greater in these modulation doped structures, as determined from SdHOs.⁶ Further work is required for a full understanding of the CR linewidth and splittings that appear in these spectra involving transitions from several occupied hole LLs.

Acknowledgements: OAM for funding from LNCMP, Toulouse (Project TSE6-105) and assistance from C.Faugeras & G.Martinez at HMFL Grenoble. DVK, AVI, KES and VIG for support from Russian Foundation for Basic Research (08-02-01126, 08-02-92503, 09-02-00752) and Russian Academy of Sciences.

References

1. R.J.H.Morris *et al. Semicond. Sci. Technol.* **19** L106 (2004).
2. B.Rößner, G.Isella and Hans von Känel *Appl. Phys. Lett.* **82**, 754 (2003).
3. V.Ya.Aleshkin *et al. Physics of the Solid State* **46** 130 (2004).
4. O.Drachenko *et al. Phys. Rev. B* **79**, 073301 (2009).
5. R.Winkler, M.Merkler, T.Darnhofer, U.Rössler *Phys.Rev.B* **53**, 10858 (1996).
6. B.Rößner, D.Chrastina, G.Isella, H.von Känel *Appl.Phys.Lett.* **84** 3058 (2004)
7. B.Rößner *et al. Semicond. Sci. Technol.* **22** S191 (2007)